



## Recognition and prediction of elderly thermal sensation based on outdoor facial skin temperature

Jiangnan Wang<sup>a,b</sup>, Qiong Li<sup>a,b,\*</sup>, Guodong Zhu<sup>c,d</sup>, Weijian Kong<sup>a,b</sup>, Huiwang Peng<sup>a,b</sup>, Meijin Wei<sup>c,d</sup>

<sup>a</sup> State Key Laboratory of Subtropical Building and Urban Science, South China University of Technology, Guangzhou, 510641, China

<sup>b</sup> Guangzhou Municipal Key Laboratory of Landscape Architecture, Department of Landscape Architecture, School of Architecture, South China University of Technology, Guangzhou, 510641, China

<sup>c</sup> Guangzhou Nursing Home, Guangzhou, 510900, China

<sup>d</sup> Collaborative Innovation Center for Civil Affairs of Guangzhou, Guangzhou 510900, China



### ARTICLE INFO

#### Keywords:

Thermal comfort model  
Thermal sensation vote  
Elderly population  
Facial skin temperature  
Machine learning

### ABSTRACT

The global ageing issues and climate extremes are becoming increasingly prevalent. Increasingly, elderly people may have difficulty expressing their feelings or needs for outdoor thermal comfort accurately and promptly. Therefore, it is crucial to find a reliable method for them to evaluate their thermal comfort. This study aims to explore the use of infrared images for this purpose. Experiments were conducted outdoors in the Home for the Aged Guangzhou in summer through thermal environment measurements and questionnaire surveys. The results show that the elderly are unresponsive to hot environments. The preference for wind speed changes was significant, compared to air temperature, relative humidity and solar radiation. Experiments were conducted to construct six machine learning models by inputting the local skin temperature (forehead, eye, nose, cheek and chin) of the face of an elderly person and Thermal Sensation Vote as the output parameter. The experimental results showed that the facial skin temperature of an individual can be used as an indicator of their thermal sensation. And the best performing model is Random Forest, an area under the curve value of 0.889 was achieved. This paper also discusses the selection of measurement site. The nose, a key area on the face, plays a crucial role in operating the proposed method. The results of this work may provide a theoretical basis for the dynamic monitoring of thermal sensations using facial skin temperature, which may contribute to the development of useful strategies for improving the thermal comfort of elderly populations in harsh environments.

## 1. Introduction

By the year 2050, the United Nations predicts that almost a third of the global population will be 65 years of age or older [1]. The populations of several countries, including Japan, Italy, Greece, Portugal, and Germany, already have unprecedentedly high average ages. China, the United States, France, and other countries are also experiencing rapid aging trends. The proportion of the population aged 60 and older in China is expected to reach 18.7% by 2022 and 30% by 2040 [2]. Considering the global aging problem, it becomes increasingly important to address the needs of vulnerable elderly populations.

Studies have shown that engaging in regular outdoor activities can help delay certain effects of aging, improve chronic disease symptoms, and enhance overall happiness among the elderly [3–6]. Guangzhou,

China is situated in a hot, humid region with an extended summer season and a particularly harsh climate [7], which poses significant risks to senior citizens engaging in outdoor activities. It is imperative to comprehensively understand the outdoor thermal comfort requirements and potential risks faced by elderly individuals in hot and humid areas such as Guangzhou. By addressing these factors, measures can be taken to protect their health and safety while enabling them to lead active and fulfilling lives.

### 1.1. Current status of thermal comfort research in elderly populations

Existing thermal comfort evaluation models were mostly constructed using college students as subjects. Examples include PMV [8], SET\* [9], UTCI [10], etc. However, some studies have shown that the thermal

\* Corresponding author. State Key Laboratory of Subtropical Building and Urban Science, South China University of Technology, Guangzhou, 510641, China.  
E-mail address: [arliqiong@scut.edu.cn](mailto:arliqiong@scut.edu.cn) (Q. Li).

sensations experienced by older people differ substantially from those of younger people. For example, in a study comparing the differences in outdoor thermal sensations between two groups aged 71–76 years and 21–30 years, Natsume et al. [11] found that the sensitivity of elderly people to thermal sensation decreases with age. According to Schellen et al. [12], the elderly tend to prefer warmer environments more than the young. Experiments conducted by Taylor et al. [13] demonstrated that the elderly require stronger thermal stimuli to produce the same thermal feedback as younger individuals. Krüger et al. [14], Baquero et al. [15], Lai et al. [16], Jiayan et al. [17] and Yang et al. [18] similarly determined that elderly individuals tend to be less sensitive to temperature than youths. Only when the environment is extremely harsh do elderly people take protective measures. This also means that elderly people are less likely to notice changes in the environmental climate than other age groups [19–21]. Takafumi et al. [22] found that thermoregulation in the elderly is more delayed than in young people as evidenced by their body temperatures responding to changing thermal environmental conditions. Additionally, Cedeno et al. [23] revealed an association between thermal discomfort and cognitive decline in elderly individuals.

Given the differences between the elderly and the young, it is not appropriate to directly apply findings from studies on younger age groups to the elderly populations when attempting to describe their thermal sensations accurately. There is a critical need for outdoor thermal comfort research that specifically targets the elderly to ensure their well-being and safety in different thermal environments.

Research on thermal comfort for the elderly has also predominantly focused on indoor environments. As early as 1970, Fanger et al. [24] conducted experiments with 128 subjects to validate the predicted mean vote (PMV) model for indoor thermal comfort in the elderly. They highlighted the differences in thermal comfort between the elderly and younger individuals. As the global population continues to age, health issues relevant to the elderly have garnered significant research attention [25,26]. Consequently, the thermal comfort needs of the elderly have become an area of strong interest for researchers. For instance, Jiang et al. [27] investigated the thermal comfort of residents in a Japanese home for the elderly using a questionnaire to find that they had relatively low sensitivity to indoor air humidity and a poorer perception of the vertical temperature difference of their bodies. Similarly, in a study focusing on elderly individuals in the Mediterranean continental climate of Spain, María et al. [28] found that the sensitivity of elderly people to temperature changes was lower than the predicted value of PMV. Jiao et al. [29] observed that when elderly people were dissatisfied with the indoor thermal environment, they were more inclined to adapt to the conditions through self-regulation (e.g., reducing physical activity, increasing water intake, adjusting clothing) than younger people.

There have been fewer studies on outdoor thermal environments for older adults compared to indoor thermal environments. Most studies on this subject focus on the thermal comfort range of the elderly when thermal sensation is neutral (TSV between -0.5 and 0.5) in different climatic zones. For example, Xi et al. [30] and Xu et al. [31] found that the thermal comfort range in cold regions tends to be wider than that in hot regions. Larriva and Higueras [32] discovered that the thermal neutral temperatures of older people in hot regions are significantly higher than those in other climatic regions. In a study conducted in the Tibetan Plateau, Yao et al. [33] observed differences in the thermal comfort of physiological equivalent temperature (PET) between the elderly in different climatic regions and those in Lhasa, especially in terms of the lower limits.

Some studies have also investigated how modifying the layouts of outdoor spatial environments and enhancing local microclimates can reduce the risks associated with outdoor activities for the elderly. Li et al. [34], for example, selected eight different types of spaces in Martyrs' Park in Changsha to explore the thermal comfort of elderly people in various spaces, obtaining targeted findings for the elderly

population of the area. Ma et al. [35] investigated the relationship between thermal perception, age, and chronic diseases of the elderly in Xi'an Park. Based on meteorological characteristics, consultations with elderly residents, and reports of thermal perceptions, they proposed optimal design strategies for open spaces that would be suitable for the elderly.

## 1.2. Current status of research on skin temperature and thermal comfort

The outdoor thermal environment is a dynamic and complex system that is difficult to quantitatively or precisely improve based solely on subjective descriptions of human thermal comfort. Incorporating physiological indicators may allow for more objective evaluations of thermal comfort. Ma et al. [36], for example, conducted research on elderly individuals in Xi'an to investigate changes in EEG (Electroencephalogram) signal properties and their correlation with thermal perception. They found that the  $\alpha$  wave of the right cerebral hemisphere, particularly the O2 channel of the occipital lobe, can be utilized to identify elderly adults' thermal comfort levels. Wang et al. [37] investigated the relationship between blood pressure, respiratory rate, oxygen saturation, and heart rate with thermal perception in elderly people, and developed two regression models for cold and warm exposures accordingly. Chihye et al. [38] explored the relationship between skin temperature and heat perception of elderly individuals in a Korean climate chamber, and noted that cheek and dorsal hand skin temperatures were helpful in predicting heat perception.

Skin temperature has proven to be a highly effective, accurate, and easily measured physiological indicator for predicting human thermal comfort. Numerous studies have demonstrated that skin temperature, especially that of the face, can reliably reflect thermal sensations [39–41]. The non-invasive nature of infrared cameras allows for swift and simple measurements of facial skin temperature without the need for clothing removal, making it a practical method for evaluating thermal comfort [31,42]. For instance, Pavlin et al. [43] found a strong correlation between facial skin temperature extracted by infrared thermal imagers and human thermal comfort. Simha et al. [44] used an infrared thermal imager to extract facial skin temperature and built a thermal comfort model through machine learning, achieving 76% accuracy. Seungjae et al. [45] used frame glasses equipped with infrared probes to collect facial skin temperature and proposed a thermal comfort prediction model based on the Markov Model (HNN), which showed an accuracy of 81%.

For the elderly, declining cognitive ability and physiological functions can hinder the ability to accurately perceive or judge the thermal environment, leading to potential risks during heatwaves. Facial skin temperature extraction by infrared thermography can minimize potentially negative psychological impacts of invasive thermometry equipment and increase the accuracy of the results. As discussed above, the elderly and the young have very different levels of skin temperature sensitivity and perception [46,47] and elderly individuals are at increased danger of health problems due to heat waves. The elderly cannot correctly and objectively judge the thermal environment due to the decline in cognitive ability and physiological function, which increases the danger of the elderly being affected by the heat wave. Measuring the links between facial skin temperature and thermal sensation in elderly individuals may be extremely useful, as it provides an objective and reliable means of assessing thermal comfort, particularly for those who may be unable to do so subjectively.

In summary, most of the current research on thermal comfort for the elderly focuses on indoors with a single environmental change. Research in complex outdoor thermal environments has mostly explored the thresholds of existing thermal comfort indicators (e.g., UTCI, PET, SET\*, etc.). In this experiment, thermal sensations of the elderly were combined with physiological indicators (skin temperature) of the elderly. And methods such as infrared thermography and machine learning are used to construct a model for predicting thermal sensation of the elderly

by facial skin temperature.

### 1.3. Aim of this study

An experiment was conducted at the Home for the Aged Guangzhou for the purposes of this study. Whether facial skin temperature can be used to accurately evaluate the thermal sensation of elderly individuals was investigated by means of thermal environment measurements, questionnaire surveys, and infrared thermography data. Key areas of the face were screened to develop a model for predicting outdoor thermal comfort in the summer for elderly people in hot and humid regions. This work can provide a theoretical basis for dynamic monitoring of summer outdoor thermal comfort in older adults. It can help to detect thermal discomfort in elderly people in time and reduce their exposure to heat waves.

## 2. Methods

### 2.1. Study site

Guangzhou has an oceanic subtropical monsoon climate characterized by warm, rainy, and sunny conditions, with a lengthy summer and brief frost season. According to climate data from 2012 to 2022, July and August are typically the hottest months, with an average monthly maximum temperature of 30.5 °C and an extreme maximum temperature of 41.4 °C. The average relative humidity in summer varies between 75.6 and 85.0% [48].

The Home for the Aged Guangzhou was selected as the location for this experiment. It is situated in China's Guangdong Province in Zhonglutan Town, Baiyun District, Guangzhou City. An outdoor space with a suitable climate near to the home and frequented by the residents was selected to distribute a questionnaire survey to assess the outdoor thermal comfort of the elderly individuals under various thermal conditions. The experiment took place during a sunny summer period, specifically on August 12, 2022 (morning) and August 13, 13, 14, 16, 17, 18 and 19 (all day) totaling 6.5 days. Measurements were taken at six sites, as shown in Fig. 1.

### 2.2. Research subjects

The sample size was determined using G\*Power 3.1.9.7 [49,50]. Given the utilization of an in-subject design, each participant completed the entire experiment. Repeated measures ANOVA served as the statistical model, following the methodology proposed by Lan and Lian [51]. According to Cohen's guidelines [52], with an effect size ( $f$ ) set at 0.8, a significance criterion ( $\alpha$ ) of 0.05, and a statistical power ( $1-\beta$ ) of 0.8, the recommended sample size is at least 7, as illustrated in Fig. 2.

The Home for the Aged Guangzhou exhibited a relatively stable population. Through an extended period of longitudinal investigation, it has been observed that, due to the COVID-19 pandemic and the physical

condition of elderly, there are presently 34 elderly individuals engaging in outdoor activities for an extended duration. This group comprises 14 males and 20 females. Therefore, we recruited these 34 elderly people. The minimum sample size was met.

The individuals' mean age was 83 and their mean body mass index (BMI) was 22.3 kg/m<sup>2</sup> at the time of their participation, details of which are shown in Table 1. Subjects were mainly selected from older adults who were regularly active outdoors. Each of the elderly has been living in Home for the Aged Guangzhou for more than ten years. Short sleeves, long pants, socks, and summer sports shoes were worn. According to ISO 9920 (2007), the clothing's thermal resistance (clo) was calculated to be 0.57clo [53].

### 2.3. Questionnaire setting

The first part of the questionnaire collected basic personal information including age, gender, height, weight, and dress. The second part investigated thermal sensations, thermal comfort, and preferences across each of the four thermal environment parameters (air temperature, relative humidity, solar radiation intensity, and wind speed). The second part of questionnaire are shown in Fig. 3.

### 2.4. Instrumentation and parameters

In this study, high performance thermal imaging camera (Testo 872 thermal imager) was used to collect surface temperatures of face from the subjects. The description of this thermal imaging camera is listed in Table 2. The thermal camera employed in this study boasts a resolution of 320 × 240 pixels and features an integrated 3.1-megapixel visible digital camera. This enables the clear delineation of distinct face regions, resulting in the acquisition of more detailed information and improved accuracy of temperature readings. The entire experiment was conducted under the shade of a tree to avoid heatstroke among the elderly and to avoid direct sunlight on the infrared thermal imager. The human emissivity was selected as 0.98 with reference to reference [54]. (Infrared imaging technology uses the principle that the reflectivity of a material changes with temperature to test the temperature distribution on the surface of an object.) Emissivity is the ratio of the energy radiated from the surface of an object to the energy radiated from a blackbody at the same temperature. The emissivity of various substances is determined by the qualities of the object itself, so the energy radiated outward will be different for different substances at the same ambient temperature [55]. The device was fixed at the same height as the face of an elderly person in a sitting position and data were collected for an experimentally defined period of time.

During the experiment, observations were collected at 1-min intervals for thermal-environmental parameters including air temperature ( $T_a$ ), relative humidity ( $RH$ ), wind speed ( $v$ ), and black globe temperature ( $T_g$ ). Facial skin temperatures were collected for the participants every 10 min using an infrared thermal imager. The instrument collected

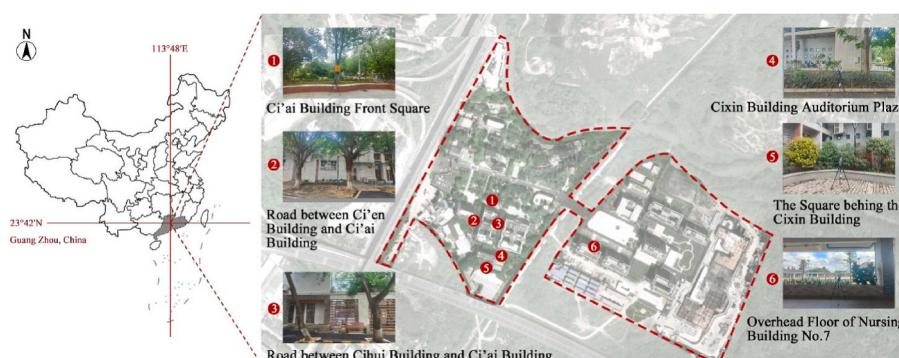


**Fig. 1.** Distribution map of measuring points in Home for the Aged Guangzhou.

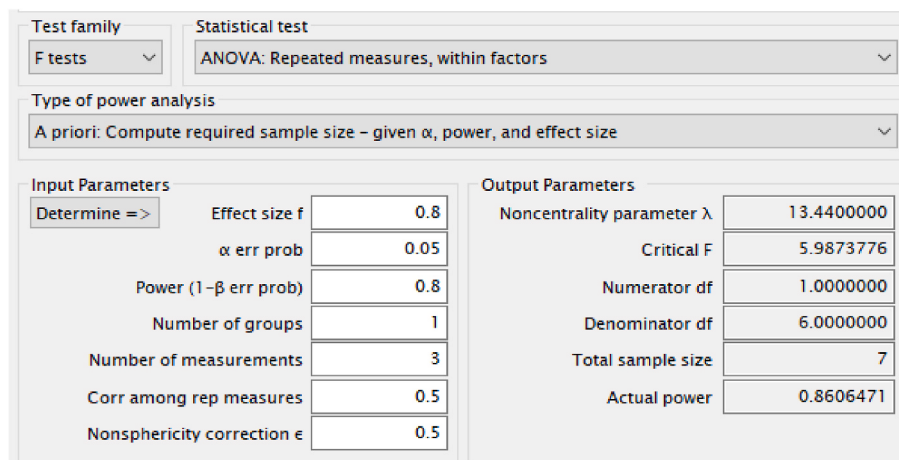


Fig. 2. Calculation of required sample size with G\*Power3.1.9.7.

**Table 1**  
Detailed information on subjects.

Genders	Sample size	Age	Weight (kg)	Height (cm)	BMI ( $\text{kg}/\text{m}^2$ )
Male	14	80	58.3	163.3	21.9
Female	20	85	52.8	150.6	23.3

measurements from a 1.1 m position, i.e., near the height of the face of an elderly person in a sitting position.

The air temperature ( $T_a$ ) and relative humidity ( $RH$ ) were recorded on a HOBO MX2302A data recorder (ONSET, USA) and wind speed ( $v$ ) and black sphere temperature ( $T_g$ ) data were recorded with a HD32.3 thermal environment monitor (Delta OHM, Italy). The measuring range, accuracy, and data acquisition frequency of all test instruments are listed in Table 3; all comply with ISO7726 (1998). The mean radiation temperature ( $T_{mrt}$ ) can be calculated as follows:

$$T_{mrt} = \left[ (T_g + 273.15)^4 + \frac{1.1 \times 10^8 \times v^{0.6}}{\varepsilon_g \times D^{0.4}} \times (T_g - T_a) \right]^{\frac{1}{4}} - 273.15 \quad (1)$$

where:  $T_g$  is the black globe temperature ( $^{\circ}\text{C}$ );  $\varepsilon_g$  is the black globe radiation coefficient, the value of which is 0.95 in this case;  $D$  is the

**Table 2**  
Skin temperature measuring instruments.

Instrument	Range	Resolution	Thermal sensitivity	Accuracy
Testo 872 thermal imager	-30°C-650 °C	320 (V)x240 (H) pixels	<0.05 °C	±2 °C

**Table 3**  
Test instrument and accuracy.

Instrument and model	Measured parameters	Measuring range	Instrument precision	Collection Frequency
HOBO MX2302A	Air temperature Relative humidity	-40°C-70 °C 0%-100%	±0.02 °C (0°C-50 °C) ±2.5% (10°C-90 °C)	1min (automatic)
HD 32.2 thermal index meter	Wind speed Black globe temperature	0 m/s-5m/s -10°C-100 °C	±0.15 m/s Class 1/3 DIN	1min (automatic)

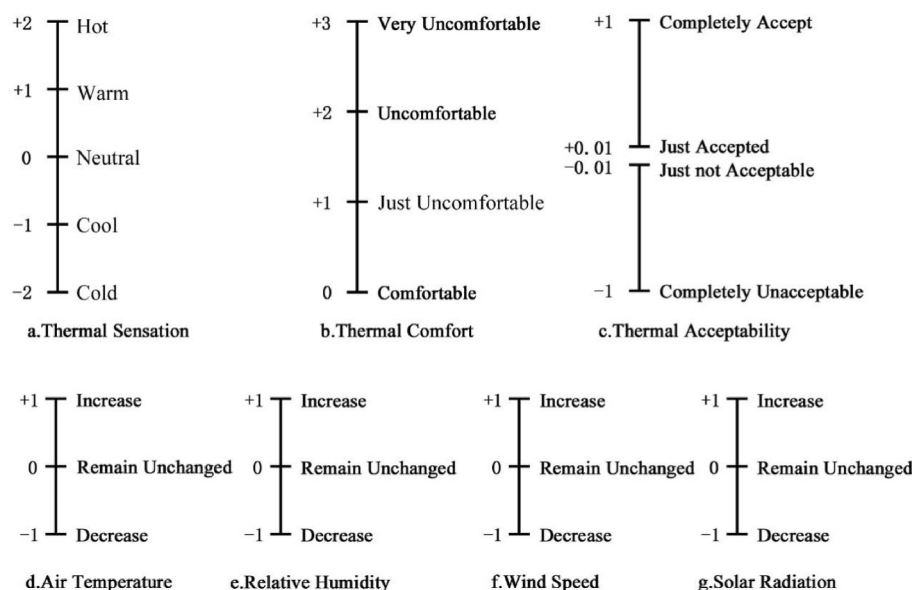


Fig. 3. Thermal comfort questionnaire.

diameter of the black globe (m), which is 0.15 m;  $v$  is the wind speed (m/s);  $T_a$  is the air temperature (°C).

## 2.5. Experimental procedure

The experimental procedure is shown in [Figs. 4 and 5](#) displays images of the test site. In total, 611 sets of data from the thermal comfort questionnaire and participants' facial infrared photographs were collected. A similar order of magnitude in the thermal comfort experiments of Larissa et al. [56], Wang et al. [37], Ma et al. [36]. Therefore, the results obtained from the 611 data collected in this paper are plausible.

The first part of the experiment was conducted from 8:20 to 10:10, while the second part covered the hours from 14:20 to 16:10. Before commencing the experiment, a standard 10-min break was given to all participants to eliminate any variations in their pre-experimental thermal experiences. To simulate the thermal comfort experiences of the elderly under different conditions, the participants engaged in a sequence of five activities, in order as exercising, walking, sitting, exercising, and sitting, each lasting 10 min in the morning part of the experiment. In the afternoon part, considering the more extreme temperature conditions, the order of activities was adjusted to exercising, sitting, walking, sitting, then exercising. The participants were led through designated health exercises during the "exercising" activity; they were guided along a designated route around the test site for the "walk" activity. After each activity, there was a 10-min rest interval during which the participants completed thermal comfort questionnaires.

## 2.6. Data processing

### 2.6.1. Data cleaning and preprocessing

[Fig. 6](#) shows the process of extracting the facial skin temperature from thermal infrared images of an elderly person. The thermal infrared images were superimposed with visible-spectrum photographs by key point calibration in Testo software to extract forehead, eye, cheek, nose, and chin temperatures from the participants, denoted as F, E, C, N, and H, respectively. Eye temperatures and cheek temperatures were averaged over the left and right sides.

There were 366 "neutral" samples, 147 "warm" samples, and 98 "hot" samples among the 611 sets of raw data. Since the experiment was collected outdoors in Guangzhou during the summer months, there was no colder climate during the normal outdoor activity hours of the elderly. Therefore, the sample sizes for "cool" and "cold" were not collected in this experiment. There is an imbalance between the three sample sizes in the raw data. This imbalance can be attributed to the necessity of prioritizing the physical safety of the elderly participants, limiting their exposure to harsher conditions for extended periods. To address the data imbalance, oversampling was applied to the "hot" and

"warm" samples using the Synthetic Minority Oversampling Technique (SMOTE) with reference to previous studies [54,57–59]. The SMOTE technique was operated in two main steps. First, the K-nearest neighbors are determined for each sample in the minority class ("hot" and "warm"). Second, new minority samples were generated by random linear interpolation using these K nearest neighbors. This process was repeated until the oversampled data was balanced. The final oversampled datasets include 1127 sets of data comprising 366 "neutral", 386 "warm", and 375 "hot" samples. The oversampled data is only used for machine learning model construction. For the analysis of the current state of thermal comfort of the elderly, the original 611 data were still used.

### 2.6.2. Hyperparameter optimization and cross-validation

The most accurate model for predicting thermal sensation in the elderly was determined by comparison against six commonly used machine learning algorithms: The random forest (RF) classifier, support vector machine (SVM), decision tree (DT) classifier, logistic regression (LR), Ada boost (AB) classifier, and gradient boosting (GB) classifier. The skin temperature of the entire face was utilized as the input feature, and 1127 data points were employed after oversampling. The output label was the projected human thermal sensation vote. The output value was compared with the real thermal sensation vote (TSV) to assess the prediction effect.

The hyperparameters for each of the six methods listed above were adjusted using a grid search, and their respective values are given in [Table 4](#). To ensure the reliability of the model training, the data was split into 80% for the training set and 20% for the test set. The model's accuracy was also assessed using the five-fold cross-validation method.

### 2.6.3. Selection of evaluation criteria

In this paper, AUC, accuracy and learning curve are used as evaluation criteria. The Area Under the Curve (AUC) and Receiver Operating Characteristic (ROC) curves were chosen used to assess the proposed model's effectiveness [54,60]. The ROC curve plots the "true positive rate" (the ratio of predicted positive samples to all positive samples in the sample) on the vertical coordinate against the "false positive rate" (the proportion of predicted negative samples to actual negative samples) on the horizontal coordinate. The AUC is the area enclosed by the ROC curve. An AUC value closer to 1 indicates a more effective classifier. The AUC is a useful metric for assessing a model's performance in classification problems as well as its generalization ability. Accuracy refers to the proportion of samples correctly classified by the classifier to the total number of samples. The overall performance of the classifier can be intuitively understood.

In order to evaluate whether the model has underfitting or overfitting problems in the hyperparameter tuning process, this paper uses learning curves [61] to make judgements. (The results of the learning curve are shown in 3.4.1.) The learning curve is the curve of the model's

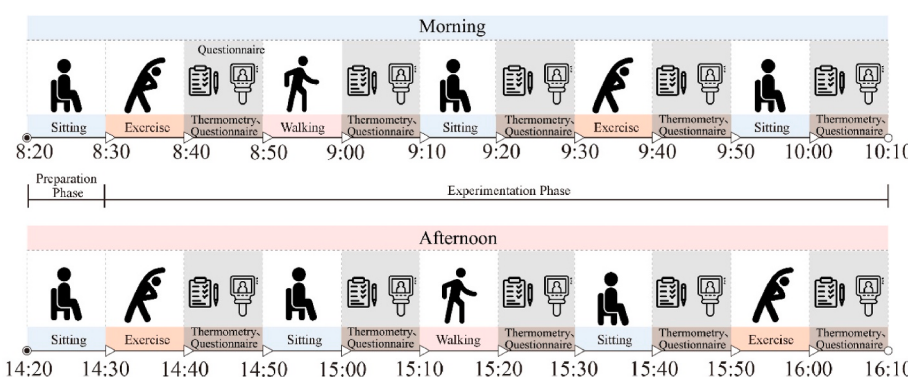
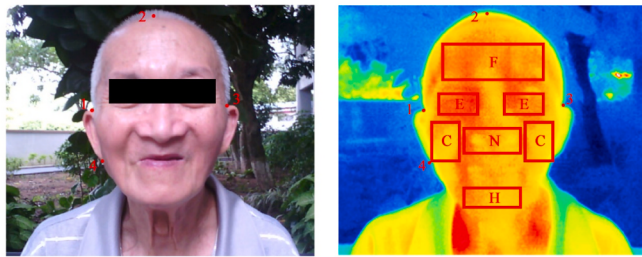


**Fig. 4.** Experimental process.



Fig. 5. Photos of experimental scene.



● Key points for calibration of thermal infrared images and visible photographs.  
□ Extraction area  
forehead-F; eye-E; nose-N; cheek-C; chin-H

Fig. 6. Facial skin temperature measurement.

**Table 4**  
Hyperparameters involved in grid search.

Algorithm	Hyperparameter	Values
Support Vector Machine (SVM)	Kernel	rbf, linear, poly
	C	0.01, 0.1, 1, 10, 100
Random Forest Classifier (RF)	n_estimators	10, 20, 30, 40, 50, 60, 70, 80, 90, 100
	max_depth	1, 2, 3, 4, 5, 6, 7, 8, 9, 10
	min_samples_leaf	2, 3, 4, 5, 6, 7, 8, 9, 10
Logistic Regression (LR)	solver	lbfgs
	penalty	l1, l2
	C	0.001, 0.01, 0.1, 1, 10, 100, 1000
Ada Boost Classifier (AB)	n_estimators	10, 20, 30, 40, 50, 60, 70, 80, 90, 100
	learning_rate	0.0001, 0.001, 0.01, 0.1, 1, 10
Decision Tree Classifier (DT)	max_depth	2, 3, 4, 5, 6, 7, 8, 9, 10
	criterion	gini, entropy, log_loss
	splitter	best, random
Gradient Boosting Classifier (GB)	n_estimators	10, 20, 30, 40, 50, 60, 70, 80, 90, 100
	learning_rate	0.0001, 0.001, 0.01, 0.1, 1, 10
	min_samples_split	1, 2, 3, 4, 5, 6, 7, 8, 9, 10
	max_depth	1, 2, 3, 4, 5, 6, 7, 8, 9, 10

\*Kernel is the kernel type to be used in the algorithm; C is the regularization parameter; N\_estimators is the number of trees in the forest; Max\_depth is the maximum depth of the tree; Min\_samples\_leaf is the minimum sample of leaf nodes; Solver is the optimization method for the loss function; Penalty is the penalty term used in the model; Learning\_rate is the learning rate of the model; Criterion is the method for calculating impurity; Splitter is the node splitting principle; Min\_samples\_split is the minimum number of samples required to split internal nodes.

score change on the training and validation sets under different data volumes, and the state of the model can be judged by whether the curve converges or not.

### 3. Results

#### 3.1. Outdoor thermal environment level of home for the Aged Guangzhou

The background meteorological data during the experimental period of the Home for the Aged Guangzhou, as shown in Fig. 7, indicated relatively consistent trends in the thermal environment parameters. During the experimental period, the mean air temperature was around 31.5 °C, the relative humidity was 73.5%, the wind speed was 1.5 m/s, and the solar radiation was 200.0 W/m<sup>2</sup>, which is typical of the summer weather in Guangzhou. The consistency of meteorological parameters during the experiment was examined by Cronbach's alpha [62]. The results show that the Cronbach's alpha for air temperature, relative humidity, wind speed and solar radiation are all greater than 0.7. This indicates the consistency of the background meteorological parameters during the experiment. However, the average temperature was low and the humidity was high due to rain in the afternoon, so only the morning part of the experiment was conducted on August 12.

#### 3.2. Status of outdoor thermal comfort in home for the Aged Guangzhou

##### 3.2.1. Thermal sensation and thermal comfort voting

The thermal sensation and thermal comfort voting of elderly people in different exercise states are shown in Fig. 8. It is evident that as the amount of exercise increases, the proportion of votes for "neutral" and "comfortable" decreases while the proportion of "warm", "hot", "slightly uncomfortable", and "uncomfortable" increases. Despite the varying levels of exercising, the majority of the participants still chose "neutral" and "comfortable" options. This is due to a decline in basal metabolism in the elderly and a weakened sensitivity to the environment [63]. By comparing Fig. 8 (a) and (b), we found that the percentage of votes for "comfortable" was greater than the percentage of votes for "neutral". This suggests that when elderly people's thermal sensation is "warm" or "hot", they still choose the "comfortable" option. This suggests that the elderly are more accepting of hot environments. The difference between the "Comfortable" and "Neutral" percentages is greatest in the "Exercising" state. The reason for this is presumably that elderly people have a slower metabolism and their actual heat production is lower than their expected heat production, making them feel satisfied. This makes the exercise state more acceptable to the thermal environment for elderly people. This is similar to the findings of Kenney et al. [64].

##### 3.2.2. Preferences for thermal environment parameters in the elderly

As shown in Fig. 9, as exercise increased, the participants tended to report preferences for lower temperatures, less radiation, and higher wind speeds. Elderly people appear to be the least sensitive to relative humidity among the parameters examined in this study. Because almost all of the elderly subjects chose to keep humidity constant. The overall proportion of preferences indicates a marked inclination towards wind

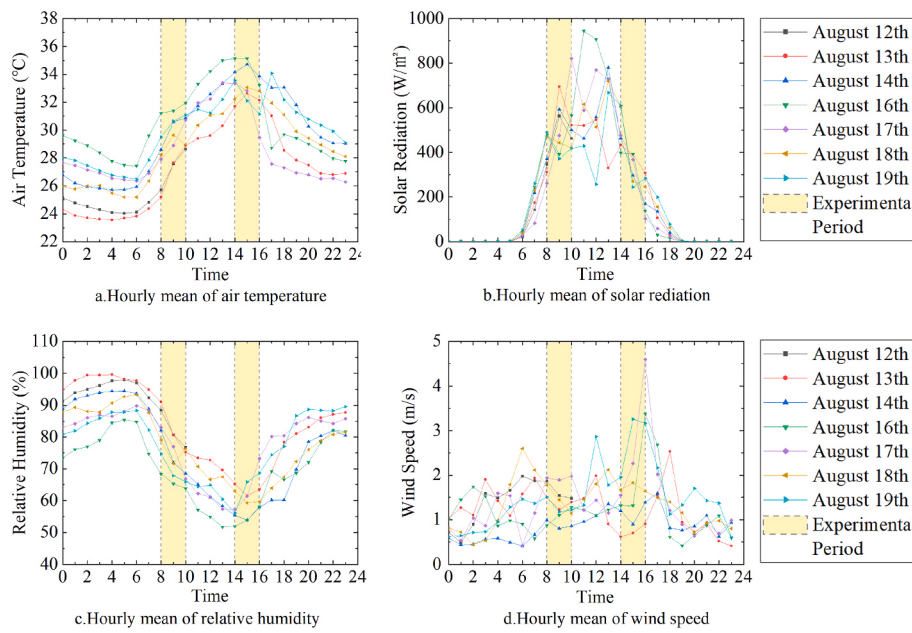


Fig. 7. Hourly average thermal environment parameters throughout experiment.

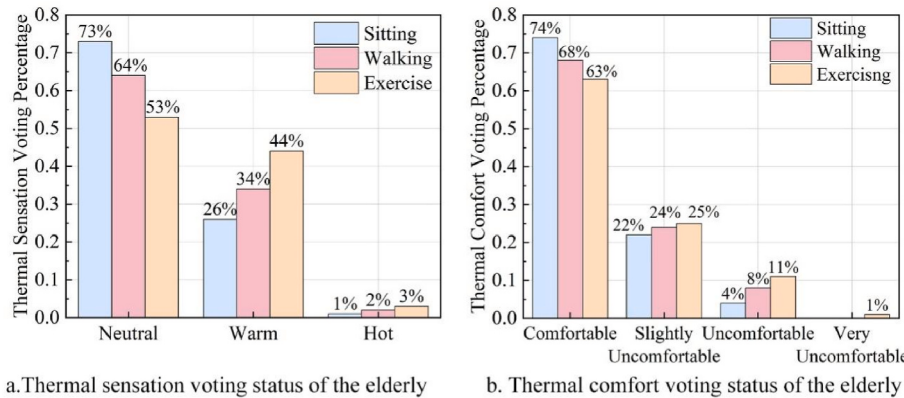


Fig. 8. Distribution of thermal sensation and thermal comfort voting in elderly participants.

speed, with a majority of the participants desiring outdoor thermal comfort to be achieved through increased air circulation. Hence, future thermal environment retrofits could be centered on ventilation improvements to cater to the preferences of the elderly.

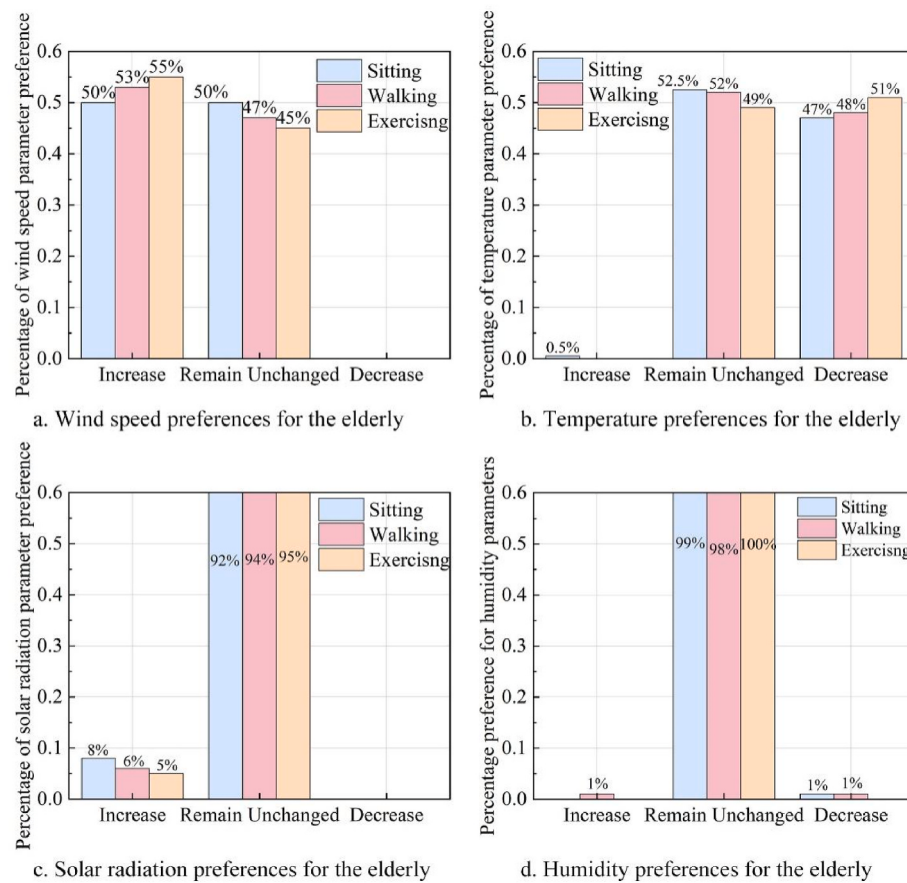
### 3.3. Facial skin temperature characteristics of the elderly

Fig. 10 and Table 5 illustrates the characteristics of skin temperature in various parts of the elderly participants' faces. When the air temperature is 26–29 °C, changes in the skin temperature of each part of the face are more consistent with the air temperature, displaying a consistent increasing trend as air temperature rises. However, once the air temperature reaches 29 °C, the temperature of all parts of the face stabilizes and no longer exhibits a proportional increase with air temperature. In addition, with the increase of temperature, the standard deviation of temperature in each part of the face gradually decreased, and the individual differences gradually decreased. The smallest standard deviation was for the eye temperature, which was 1.02 °C. The largest was the chin temperature at 1.21 °C. The average temperature of the nose exhibits a higher temperature than other parts of the face, remaining at approximately 35.1 °C. The average temperature of the cheek maintains a cooler temperature, near 34.2 °C. The nose has the

highest temperature in the maximum temperature, reaching 39.1 °C. The smallest is the chin temperature. The eye temperature is the highest among the minimum temperatures at 32.6 °C. The smallest is the cheek temperature.

The significance and effect size results of the Kruskal-Wallis test for multiple independent samples are presented in Table 6, indicating significant differences among all facial skin temperatures ( $P < 0.001$ ). To explore the variability in facial skin temperatures, effect sizes were calculated. Unlike the P-values that determine whether differences exist between groups, effect size quantifies the magnitude of differences. Cohen's values of 0.2, 0.5, and 0.8 correspond to small, medium, and large effects, respectively [65]. As shown in Table 6, the largest effect size is observed between the nose and cheeks, while the smallest effect size is between the chin and forehead. The effect sizes between the nose and other facial regions are relatively large, indicating substantial differences, with the greatest difference observed between the nose and cheeks.

Fig. 11 depicts the distribution characteristics of the elderly participants' TSV and facial skin temperatures. The facial skin temperature increases as the participant's perception of the environment leans hotter. Across all three heat sensations, the temperature variations between the eyes, cheeks, and nose are more pronounced. However, the



**Fig. 9.** Distribution of environmental parameter preferences in elderly participants.

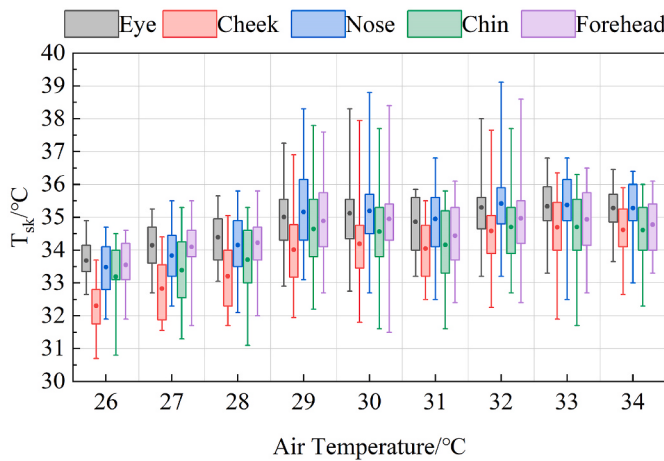


**Fig. 10.** Characteristics of skin temperature in various parts of the face.

**Table 5**  
Characteristics of skin temperature in various parts of the face.

	Eye	Cheek	Nose	Chin	Forehead
Minimum/°C	32.6	30.7	31.9	30.8	31.5
Maximum/°C	38.3	38.0	39.1	37.8	38.6
Average/°C	35.0	34.2	35.1	34.5	34.8
Standard Deviation/°C	1.02	1.18	1.18	1.21	1.14

**Table 6**  
The effect size magnitude of facial skin temperatures.

	Forehead	Eye	Cheek	Nose
Eye	0.336*			
Cheek	0.647**	0.556**		
Nose	0.694**	0.698*	0.813**	
Chin	0.335**	0.342**	0.533**	0.707**

"\*" represents  $P < 0.05$ , indicating significance at the 5% level, while "\*\*\*\*" represents  $P < 0.01$ , indicating high significance at the 1% level.

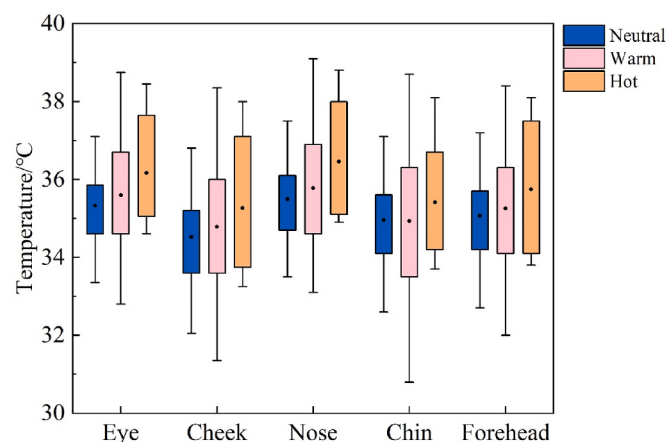


**Fig. 11.** Skin temperature at different thermal sensations.

temperature differences are relatively small and the distinction less evident between the chin and forehead for “neutral” and “warm” sensations.

When the elderly participants reported feeling “neutral”, the average nose temperature was 35.4 °C, the average eye temperature was 35.3 °C and the average cheek temperature was 34.5 °C. When feeling “warm”, the average temperature of the nose was 35.7 °C, the average temperature of the eyes was 35.6 °C and the average temperature of the cheeks was 34.8 °C. When feeling “hot”, the average temperature of the nose, eyes and cheeks were 36.5 °C, 36.1 °C, and 35.3 °C, respectively.

### 3.4. Establishment of summer thermal comfort model for the elderly

#### 3.4.1. Model selection and evaluation

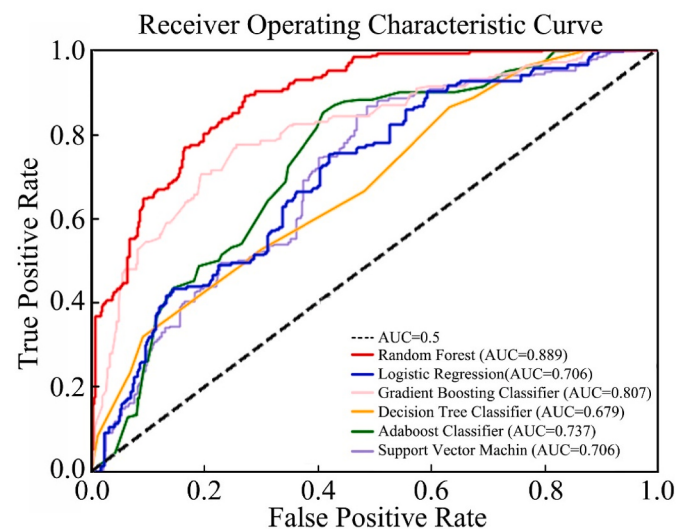
The Scikit-learn package and associated Python 3.8 routines were used in this study to train the machine learning model. Table 7 and Fig. 12 display the optimal hyperparameter findings for each machine learning algorithm.

Fig. 12 displays the ROC curves for each algorithm. The RF classifier exhibits the largest initial slope of the ROC curve, resulting in the highest AUC value (AUC = 0.889). When the “false positive rate” in the horizontal direction approaches 0, the “true positive rate” of RF is the largest, indicating its superior accuracy. Therefore, the RF classifier outperformed the other algorithms tested in this study. In addition, the hyperparameter tuning results in Table 7 show that when max\_depth is 5, n\_estimators is 100, and min\_samples\_leaf is 3 in the hyperparameters of RF, the prediction model of facial skin temperature and thermal sensation for elderly people in hot and humid regions in summer is most effective. The next most effective algorithms were the GB classifier and SVM.

From the results of the learning curve in Fig. 13, it can be seen that algorithms with good convergence (the scores of the training set and the cross-validation set reach convergence) include SVM, LR and DT. Among them, the SVM has the fastest convergence rate and reaches convergence when the sample is 700. When the sample size reaches 900, the decision tree also reaches convergence, but both algorithms end up with lower convergence values, which may have underfitting. In contrast, the RF, AB, and GB did not fully converge. But the training data values and the cross-validation values ended up within 0.05 of each other in terms of accuracy. This error is ignored with reference to Wu [66], Luo [67], and Yu [61] et al. Therefore, in this paper, the constructed models of Random Forest, Ada Boost Classifier and Gradient Boosting Classifier are also reasonable. Considering their AUC, convergence and computational speed, the RF was finally selected for the construction of the thermal

**Table 7**  
Hyperparameter tuning results.

Algorithm	Hyperparameter	AUC	Accuracy
Support Vector Machine ( SVM )	Kernel = linear C = 100	0.706	60.1%
Random Forest Classifier ( RF )	max_depth = 5 n_estimators = 100 min_samples_leaf = 3	0.889	80.6%
Logistic Regression ( LR )	solver = lbfgs penalty = 12 C = 1000	0.706	43.4%
Ada Boost Classifier ( AB )	n_estimators = 30 learning_rate = 0.1	0.737	63.9%
Decision Tree Classifier ( DT )	max_depth = 7 criterion = entropy splitter = best	0.679	80.0%
Gradient Boosting Classifier ( GB )	n_estimators = 10 learning_rate = 0.1 min_samples_split = 2 max_depth = 2	0.807	72.4%



**Fig. 12.** ROC curves of each algorithm.

sensation prediction model. The RF classifier has advantages including rapid computation, high accuracy, and the ability to measure the relative relevance of features before constructing a model. These features also align with the thermal comfort prediction models created by He Y. [54], Jiao Y. [68], and Lee Y. et al. [69].

#### 3.4.2. Critical facial screening

In practical applications, conducting measurements at multiple parts of the face can be cumbersome and challenging. This study aims to achieve more accurate predictions with fewer measurement areas by selecting key parts of the face based on the RF model. The facial regions were categorized into single, double, triple, and quadruple measurement points to assess the effects of different measurement point quantities on the test results. All feature combinations of these four categories were trained using RF and the AUC values were calculated as shown in Table 8.

As indicated by the AUC values in Table 8, the temperature of the nose appears to be the most effective measurement point when utilizing only one point, achieving an AUC value of 0.825. When two measurement points are used, the combination of the cheek and nose performs best (AUC = 0.856). When three measurement points are used, the combination of the forehead, nose, and chin performs best (AUC = 0.876). The eyes, forehead, nose, and chin were the four measurement points that appear to work best together (AUC = 0.888). The nose temperature is included in the ideal combinations of all measuring site. Furthermore, the difference in AUC values between these four combinations is small, suggesting that choosing only the nose temperature as the key area for thermal sensation prediction would be an effective option in practical applications.

## 4. Discussion

### 4.1. Facial skin temperature and thermal comfort

The experimental results show that the elderly is more receptive to thermal environments. The sensitivity was stronger for wind speed and weakest for humidity. This is the same conclusion as that of Hu's study [74]. However, Fang's study [75] in Lhasa area has a different conclusion, and his study showed that the order of thermal sensation sensitivity of the elderly in summer is temperature > wind speed > sunshine, which may be due to the difference of different climate types.

The results of this study provides strong evidence that facial skin temperature is a reliable predictor of thermal comfort in the elderly, which aligns with previous findings by Li D. [76], He Y. [54], L. I. [77],

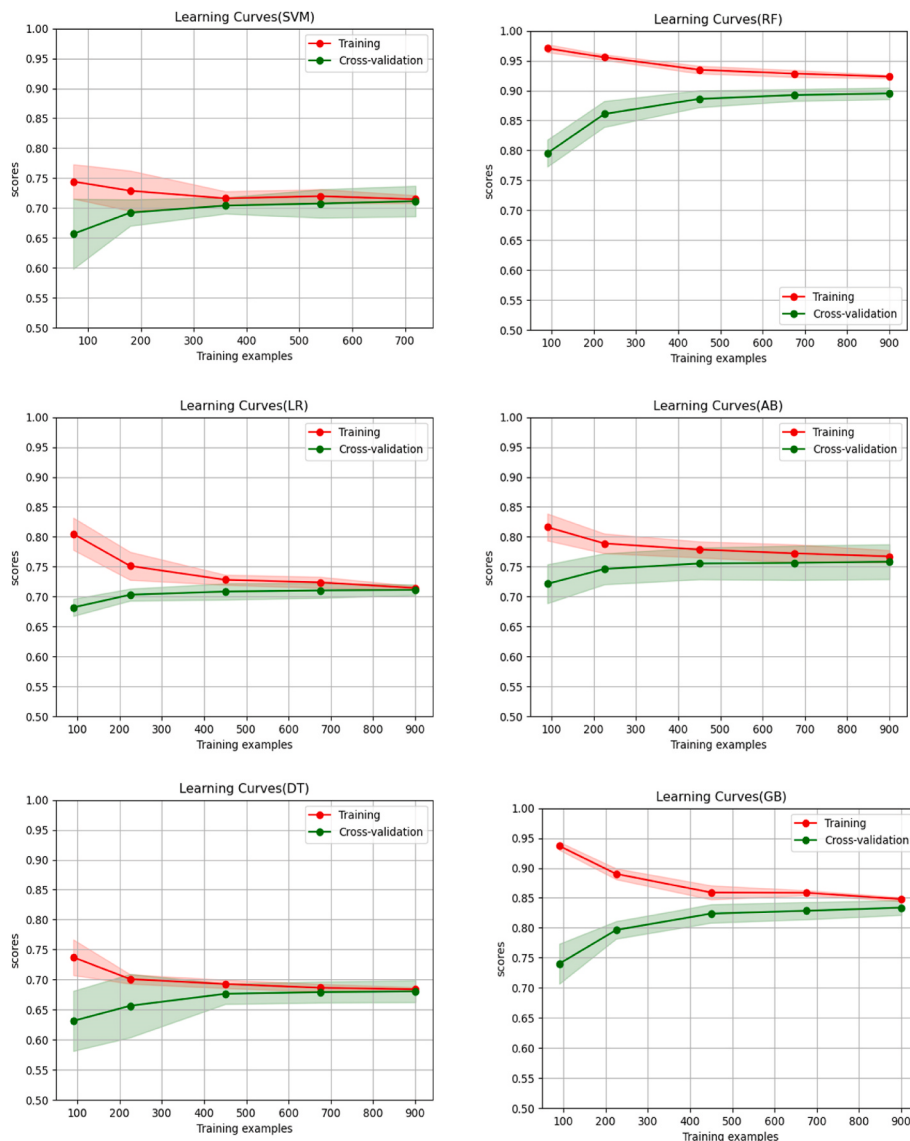


Fig. 13. Learning curve under different models.

**Table 8**

AUC values for different measurement points.

Measuring point	Quantities of key points	AUC	Measuring point	Quantities of key points	AUC
E, F, N, H	quadruple	0.888	C, N	double	0.856
C, F, N, H	quadruple	0.887	N, H	double	0.855
E, C, N, H	quadruple	0.886	E, H	double	0.853
E, C, F, H	quadruple	0.886	F, H	double	0.852
E, C, F, N	quadruple	0.884	F, N	double	0.851
F, N, H	triple	0.876	E, N	double	0.851
E, F, H	triple	0.876	C, H	double	0.849
E, N, H	triple	0.875	C, F	double	0.834
E, C, H	triple	0.873	E, C	double	0.833
C, N, H	triple	0.872	E, F	double	0.831
C, F, H	triple	0.866	N	single	0.825
E, F, N	triple	0.862	E	single	0.809
C, F, N	triple	0.860	H	single	0.807
E, C, N	triple	0.857	C	single	0.793
E, C, F	triple	0.857	F	single	0.766

\*The forehead, eye, nose, cheek, and chin are denoted as F, E, N, C, and H, respectively (see Table 9). The intent of Table 8 is to present the results for different combinations of measuring points (E, F, N, H, C) rather than emphasizing the order of inputs.

and Hardy et al. [78]. This association can be attributed to frequent lower limb tissue edema in older adults, resulting from decreased venous function [79], prolonged standing or sitting, and various chronic diseases [80], which blocks blood microcirculation at the extremities. This leads to an increase in temperature in the upper body, specifically the facial skin, making it more sensitive to changes in the external environment. Therefore, predicting thermal sensation through the objective physiological index of facial skin temperature may be very effective, especially for elderly individuals who struggle to promptly and clearly express their thermal sensations otherwise.

Table 8 show that the nose temperature is key for thermal sensation prediction, a finding consistent with Wu Y. [66], Tejedor B. [39], and Tian X. et al. [81] The specific structure of the nose, comprising cartilage and skin on the exterior and mucosa, bone and cartilage on the interior [82], plays a vital role in this regard. The nose has abundant arteriovenous anastomoses unlike other parts of the face [83,84]. This rich vascular supply allows efficient regulation of blood flow in response to changes in the environmental temperature, enabling the rapid generation or release of excess heat and making it highly sensitive to environmental changes.

**Table 9**  
Previous experimental research.

Author	Metrics	Accuracy	Input value	Output value
Andrei Claudiu et al. [70]	Accuracy	76%	left eye, right eye, nose, mouth, chin, forehead, left cheek, and right cheek	TCV
Kangji Li et al. [71]	General Acc	68.71%–91.41%	forehead, mouth, cheek, chin, nose	TSV/TCV
Yeyu Wu et al. [66]	AUC	85%	forehead, eye, nose, cheek, ear	TSV
Yingdong He et al. [54]	Accuracy	83%–96%	cheek, nose, hand	TSV
Changzhi Dai et al. [41]	Accuracy	85.1%	forehead, cheek, forearm, hand	TSV
Kuixing Liu et al. [42]	Accuracy	51.1%–91.5%	face, hand, head, upper leg, lower leg, upper arm, feet, thorax, lower arm, abdomen	TSV
Liu Weiwei et al. [72]	TP	72%	forehead, chest, upper arm, back, abdomen, elbow, hand, anterior thigh, anterior calf, foot	TSV
Blanca Tejedor et al. [39]	R2	0.8658–0.9514	nose, forehead, chin, cheekbone	TSV
Jaewon Jeoung et al. [73]	Accuracy	90.26%	eyes, nose, cheeks, mouth, and chin	TSV

#### 4.2. Thermal comfort prediction model and applications

Table 7 and Fig. 12 reveal that RF outperforms SVM, LR, AB, GB, and DT in predicting thermal comfort in the elderly based on facial skin temperature. He Y. et al. [54] also developed a thermal comfort prediction model using RF. In comparison to traditional models, machine learning-based approaches may offer superior performance [85–87]. Machine learning methods excel in efficiently learning complex and potentially non-linear relationships from data, eliminating the need for speculative relationships as seen in other methods [60]. These algorithms can derive more appropriate models based on their own data rather than relying on empirical formulas [85]. Using machine learning methods can balance the data to improve the representativeness of the category with fewer samples [88]. In this study, the main advantage of employing machine learning algorithms lies in their ability to effectively handle collinearity between facial skin temperatures. As demonstrated in the works of T. et al. [89] and Jireh et al. [90], machine learning techniques exhibit a reduced impact of covariance when constructing predictive models. Given the presence of covariance in facial skin temperatures in our study, machine learning was chosen to investigate the predictive collinearity of facial skin temperature on thermal sensation in elderly individuals. In addition, machine learning can be better combined with face recognition technology to predict human thermal comfort in real time than traditional thermal comfort analysis. This can better respond to the future trends of the Internet [91].

Previous studies on thermal comfort and skin temperature are shown in Table 9. Liu et al. [72] affixed temperature sensors to various body regions of young individuals, including the forehead, chest, upper arm, back, abdomen, elbow, hand, front thigh, front calf, and foot, encompassing 10 measurement points to construct a model. Meanwhile, Eddie et al. [92] utilized forehead temperature as an input for large-scale thermal screening, conducting a comprehensive analysis. This adhesive multi-location skin temperature collection approach potentially promises heightened accuracy. However, due to the constrained mobility of elderly individuals and the intricacies of outdoor environments, adopting infrared technology for measuring facial skin temperature emerges as a more convenient and secure methodology. The face, being the body area with the lengthiest exposure time and equipped with an infrared camera, facilitates an intuitive, swift, and convenient

prediction of human thermal comfort. Non-contact temperature measurement methods mitigate the psychological impact on elderly individuals, rendering them particularly suitable for those with limited mobility. Hence, in this study, our main emphasis is on exploring facial skin temperature as a predictor for outdoor thermal comfort in elderly individuals and identifying crucial regions. In alignment with the methodologies of Wu [66], we segmented the face into multiple regions as input values to construct the model. Blanca et al.'s [39] study also embraced a similar predictive approach, utilizing facial temperature measurements to discern the neutral temperature of elderly individuals and proposing control strategies for HVAC systems.

#### 4.3. Limitation and future study

Given the current experiment, we specifically utilized facial skin temperature as the input for constructing a predictive model for thermal comfort in the elderly. In the studies conducted by He et al. [54] and Chang et al. [41], the inclusion of both facial and hand skin temperatures as inputs resulted in an increased accuracy of approximately 5%–15% compared to our experiment. However, when only facial skin temperature was employed as an input, the accuracy remained comparable to our experiment. Consequently, in subsequent research endeavors, the incorporation of hand skin temperature as an additional measurement indicator may potentially augment the model's predictive performance. Furthermore, aligning with the prevailing trend in machine learning studies, this paper adopts TSV (thermal sensation vote) as the output, consistent with established practices in prior research [66, 81, 93]. Nevertheless, it is noteworthy that some studies have opted for TCV (thermal comfort vote) as the output. For instance, Li et al. [71] developed a predictive model based on TCV, achieving an accuracy range of 68.71%–91.41%. Notably, Shahzad et al. [94] discovered that 36% of residents deemed thermal sensations other than neutral as comfortable. Therefore, in future investigations, we intend to explore the development of a predictive model specifically targeting TCV for the elderly. The findings of this study underscore the potential of facial skin temperature as a predictive indicator for outdoor thermal comfort in elderly individuals. In contrast, Jaewon et al. [73] utilized facial skin temperature as an input to predict indoor thermal sensation. However, our study exhibited a predictive accuracy approximately 10% lower than that reported by Jaewon et al. It is essential to note that the training data in Jaewon et al.'s study were collected in a controlled, steady-state indoor environment. In contrast, our data collection occurred in real outdoor conditions characterized by non-static and complex variations. Consequently, the model's universal applicability to diverse scenarios might be limited. Therefore, future research should focus on increasing the number of measurement points, extending the duration of data collection, and incorporating data collected across different seasons to enhance the model's generalization ability. In addition, the findings of this paper will be further tested and expanded in future research in more homes for the elderly and their settlements for the elderly.

This model should be used not only for thermal comfort assessment of the elderly, but also to provide strategies for retrofitting the thermal environment. The infrared thermography used in this model can be combined with active cooling measures, such as fans, in subsequent applications. Placement at outdoor activity sites where the elderly frequently rest. The infrared probe is used to measure the skin temperature of the elderly's face. Based on this information, the fan switch and wind speed are controlled to improve the thermal discomfort of the elderly.

#### 5. Conclusions

A non-contact thermal comfort prediction model for the elderly was developed in this study through an investigation of outdoor thermal comfort and facial skin temperature collection in the Home for the Aged Guangzhou. The main conclusions can be summarized as follows.

- 1) The elderly are unresponsive to hot environments. Most elderly people feel comfortable in neutral and warm environments. The elderly in hot and humid areas require less humidity changes in outdoor spaces. However, they are more sensitive to wind speed. Therefore, the current thermal comfort of the elderly can be effectively improved by a reasonable layout of the building to form ventilation corridors.
- 2) The facial skin temperature of elderly individuals changes with air temperature, but with some fluctuations. When the ambient temperature reaches 29 °C, the temperature of the facial points is basically maintained at 35 °C. Facial skin temperature increased with the perception of the elderly to the environment becomes warmer. Among them, the temperature changes of eyes, cheeks and nose were the most obvious.
- 3) A prediction model based on five machine learning algorithms was established. Considering their AUC, convergence and computational speed, the RF is recommended for thermal comfort prediction of the elderly. The RF also verified the feasibility of predicting thermal comfort in the elderly by facial skin temperature.
- 4) In the point selection of facial skin temperature measurement, nose temperature can be used to improve the accuracy of predicting thermal comfort in the elderly. The optimal two-point measurement consists of the nose and cheek, the optimal three-point measurement includes the forehead, nose, and chin, and the optimal four-point measurement includes the eyes, forehead, nose, and chin.

#### CRediT authorship contribution statement

**Jiangnan Wang:** Writing – original draft, Visualization, Validation, Methodology, Investigation, Formal analysis, Data curation, Conceptualization. **Qiong Li:** Writing – review & editing, Methodology, Funding acquisition, Project administration, Supervision. **Guodong Zhu:** Writing – review & editing, Methodology. **Weijian Kong:** Investigation, Formal analysis. **Huiwang Peng:** Investigation, Formal analysis. **Meijin Wei:** Investigation, Formal analysis.

#### Declaration of competing interest

The authors declare that they have no known competing financial interests or personal relationships that could have appeared to influence the work reported in this paper.

#### Data availability

The data that has been used is confidential.

#### Acknowledgement

This research was funded by National Natural Science Foundation of China (NSFC) (Grant No. 52178076), Guangdong Science and Technology Plan Project (Grant No. 2023A0505050125), the project funded by State Key Laboratory of Subtropical Building and Urban Science (Grant No. 2023ZB03), and Science and Technology Project of Guangzhou (Grant No. 2023B04J0121, 202206060005).

#### References

- [1] World Healthy Organization, 2022. Date, <https://www.who.int/news-room/fact-sheets/detail/ageing-and-health>.
- [2] China Census, 2021. Date, <http://www.stats.gov.cn/tjsj/tjgb/rkpcgb/>.
- [3] Michelle E. Kelly, Brian A. Lawlor, David Loughrey, Ian H. Robertson, Cathal Walsh, Sabina Brennan, The impact of exercise on the cognitive functioning of healthy older adults: a systematic review and meta-analysis, Ageing Res. Rev. 16 (2014) 12–31. <https://www.sciencedirect.com/science/article/pii/S1568163714000610>.
- [4] Dag Aarsland, Farzaneh S. Sardahae, Sigmund Anderssen, Clive Ballard, Is physical activity a potential preventive factor for vascular dementia? A systematic review, Aging Ment. Health 14 (4) (2010) 386–395. <http://europemmc.org/abstract/MED/20455113>.
- [5] E.M. Murtagh, L. Nichols, M.A. Mohammed, R. Holder, A.M. Nevill, M.H. Murphy, The effect of walking on risk factors for cardiovascular disease: an updated systematic review and meta-analysis of randomised control trials, Prev. Med. 72 (2015) 24–43. <https://www.sciencedirect.com/science/article/pii/S009174351500002X>.
- [6] K. Korpela, K. Borodulin, M. Neuvonen, O. Paronen, L. Tyrväinen, Analyzing the mediators between nature-based outdoor recreation and emotional well-being, J. Environ. Psychol. 37 (2014) 1–7. <https://www.sciencedirect.com/science/article/pii/S0272494413000753>.
- [7] Genyu Xu, Huihui Zhao, Jinglei Li, Yurong Shi, Xuming Feng, Yufeng Zhang, Multivariate thermal environment data extraction and evaluation: a neighborhood scale case in Guangzhou, China, Build. Environ. 234 (2023) 110–190. <https://www.sciencedirect.com/science/article/pii/S0360132323002172>.
- [8] Fanger, Ole Povl, Thermal comfort: analysis and applications in environmental engineering, Appl. Ergon. 3 (1972) 181, <https://doi.org/10.1177/146642407209200337>.
- [9] A. Pharo Gagge, Jan A.J. Stolwijk, Y. Nishi, An effective temperature scale based on a simple model of human physiological regulatory response, Memoir. Facul. Eng. 13 (1972) 21–36. <http://eprints.lib.hokudai.ac.jp/dspace/bitstream/2115/37901/1/1>.
- [10] Gerd Jendritzky, Maarouf Abdel, Henning Staiger, Looking for a universal thermal climate index utci for outdoor applications, Windsor Conference on Thermal Standards 5 (2001) 33–35. <https://www.researchgate.net/publication/267953388>.
- [11] Keiko Natsume, Tokuo Ogawa, Junichi Sugeno, Norikazu Ohnishi, Kazuno Imai, Preferred ambient temperature for old and young men in summer and winter, Int. J. Biometeorol. 36 (1) (1992) 1–4, <https://doi.org/10.1007/BF01208726>.
- [12] L Lisje Schellen, Wouter D. van Marken Lichtenbelt, M.G.L.C. Loomans, Jørn Toftum, Martin de Wit, Differences between young adults and elderly in thermal comfort, productivity, and thermal physiology in response to a moderate temperature drift and a steady-state condition, Indoor Air 20 (2010) 273–283, <https://doi.org/10.1111/j.1600-0668.2010.00657.x>.
- [13] Nigel A.S. Taylor, N. Kim Allsopp, David G. Parkes, Preferred room temperature of young vs aged males: the influence of thermal sensation, thermal comfort, and affect, J. Gerontol.: Series A 50A (4) (1995) M216–M221, <https://doi.org/10.1093/gerona/50A.4.M216>.
- [14] Eduardo L. Krüger, Francine A. Rossi, Effect of personal and microclimatic variables on observed thermal sensation from a field study in southern Brazil, Build. Environ. 46 (3) (2011) 690–697. <https://www.sciencedirect.com/science/article/pii/S036013231000291X>.
- [15] Higueras Garcia, Ester, María Baquero Larriva, Outdoor thermal and acoustic comfort in autumn for senior citizens in public spaces in newcastle upon tyne, United Kingdom, Biomedical Journal of Scientific & Technical Research 24 (2020). <https://biomedres.us/fulltexts/BJSTR.MS.ID.004002.php>.
- [16] Dayi Lai, Deheng Guo, Yuefei Hou, Chenyi Lin, Qingyan Chen, Studies of outdoor thermal comfort in northern China, Build. Environ. 77 (2014) 110–118. <https://www.sciencedirect.com/science/article/pii/S0360132314000869>.
- [17] Jiayan Li, Ranhao Sun, Liding Chen, Identifying sensitive population associated with summer extreme heat in Beijing, Sustain. Cities Soc. 83 (2022) 103925. <https://www.sciencedirect.com/science/article/pii/S2210670722002475>.
- [18] Jinho Yang, Insick Nam, Jong-Ryeol Sohn, The influence of seasonal characteristics in elderly thermal comfort in Korea, Energy Build. 128 (2016) 583–591. <https://www.sciencedirect.com/science/article/pii/S0378778816306326>.
- [19] Madhavi Indraganti, Kavita Daryani Rao, Effect of age, gender, economic group and tenure on thermal comfort: a field study in residential buildings in hot and dry climate with seasonal variations, Energy Build. 42 (3) (2010) 273–281. <https://www.sciencedirect.com/science/article/pii/S0378778809002175>.
- [20] Henrique Andrade, Maria-João Alcoforado, Sandra Oliveira, Perception of temperature and wind by users of public outdoor spaces: relationships with weather parameters and personal characteristics, Int. J. Biometeorol. 55 (5) (2011) 665–680, <https://doi.org/10.1007/s00484-010-0379-0>.
- [21] Katarzyna Lindner-Cendrowska, Krzysztof Blażejczyk, Impact of selected personal factors on seasonal variability of recreationist weather perceptions and preferences in Warsaw (Poland), Int. J. Biometeorol. 62 (1) (2018) 113–125, <https://doi.org/10.1007/s00484-016-1220-1>.
- [22] Takafumi Maeda, Toshio Kobayashi, Kazuko Tanaka, Akihiko Sato, Shin-Ya Kaneko, Masatoshi Tanaka, Seasonal differences in physiological and psychological responses to hot and cold environments in the elderly and young males, in: Elsevier Ergonomics Book Series, 3, Elsevier, 2005, pp. 35–41. Tochihara, Yutaka and Tadakatsu Ohnaka, <https://www.sciencedirect.com/science/article/pii/S1572347X05800072>.
- [23] J.G. Cedeño Laurent, A. Auid-Orcid Williams, Y. Ouhote, A. Zanobetti, J.G. Allen, J.D. Spengler, Reduced cognitive function during a heat wave among residents of non-air-conditioned buildings: an observational study of young adults in the summer of, PLoS Med. 7 (2016) 1549–1676, <https://doi.org/10.1371/journal.pmed.1002605>.
- [24] Fanger, Ole Povl, Thermal Comfort: Analysis and Applications in Environmental Engineering, 1972. <https://www.cabdirect.org/cabdirect/abstract/19722700268>.
- [25] X.U. Bi-xia, Qiong Li, Hiroshi Yoshino, Pei-jie Tang, U. Yanagi, Kenichi Hasegawa, Naoki Kagi, The survey and field measurements of the summer indoor environment of urban and rural elderly residential buildings in Guangzhou, South Architecture 1 (2021) 89–94. <http://nfjz.arch.scut.edu.cn/CN/10.3969/j.issn.1000-0232.2021.01.089>.



- temperatures recognition, *Build. Environ.* 246 (2023) 110956. <https://www.sciencedirect.com/science/article/pii/S0360132323009836>.
- [72] Weiwei Liu, Zhiwei Lian, Qihong Deng, Use of mean skin temperature in evaluation of individual thermal comfort for a person in a sleeping posture under steady thermal environment, *Indoor Built Environ.* 24 (4) (2014) 489–499, <https://doi.org/10.1177/1420326X14527975>.
- [73] Jaewon Jeoung, Seunghoon Jung, Taehoon Hong, Minhyun Lee, Choongwan Koo, Thermal comfort prediction based on automated extraction of skin temperature of face component on thermal image, *Energy Build.* 298 (2023) 113495. <https://www.sciencedirect.com/science/article/pii/S0378778823007259>.
- [74] Xiaoshan Fang, JingWen Hu, Study of the outdoor thermal comfort threshold of elderly people in hot and humid regions in summer, *South Architecture* 2 (2019) 5–12. <https://kns.cnki.net/10.3969/j.issn.1000-0232.2023.07.005>.
- [75] Haidong Fang, Study on classification of typical outdoor activity space of the elderly in Lhasa (in Chinese), *Urban. Archit.* 33 (2019) 34–35. <https://kns.cnki.net/10.19892/j.cnki.csjz.2019.33.013>.
- [76] Da Li, Carol C. Menassa, Vineet R. Kamat, Non-intrusive interpretation of human thermal comfort through analysis of facial infrared thermography, *Energy Build.* 176 (2018) 246–261. <https://www.sciencedirect.com/science/article/pii/S0378778818309629>.
- [77] L.I. Crawshaw, E.R. Nadel, J.A.J. Stolwijk, B.A. Stamford, Effect of local cooling on sweating rate and cold sensation, *Pflügers Archiv* 354 (1) (1975) 19–27, <https://doi.org/10.1007/BF00584500>.
- [78] Hardy, J. D., and T. W. Oppel. Studies in Temperature Sensation. Iii. The Sensitivity of the Body to Heat and the Spatial Summation of the End Organ Responses.0021-9738. <https://www.jci.org/articles/view/100879>.
- [79] H.W. Thaler, S. Pienaar, G. Wirnsberger, R.E. Roller-Wirnsberger, Bilateral leg edema in an older woman, *Z. Gerontol. Geriatr.* 48 (1) (2015) 49–51, <https://doi.org/10.1007/s00391-013-0557-x>.
- [80] Burton D. Rose, Pathophysiology and etiology of edema-li, *Morgan & Claypool Life Sciences* 5 (2010) 345–358. <https://www.uptodate.com/contents/pathophysiology-and-etiology-of-edema-in-adults>.
- [81] Tian, X., R. Xu, and W. Liu. Facial Skin Temperature and Overall Thermal Sensation of Sub-Tropically Acclimated Chinese Subjects in Summer.0306-4565 (Print). <https://www.sciencedirect.com/science/article/pii/S0306456522002364>.
- [82] H.N. Barnett, Structure and diseases of the nose and throat; anatomy and physiology of the nose, *Nurs. Mirror Midwives J.* 83 (1946) 113. <https://europepmc.org/article/MED/20986499>.
- [83] T.K. Bergersen, A search for arteriovenous anastomoses in human skin using ultrasound Doppler, *Acta Physiol. Scand.* 2 (1993) 195–201. <https://pubmed.ncbi.nlm.nih.gov/8475746/>.
- [84] Miyaji, A., S. Hayashi, and N. Auid-Orcid Hayashi. Regional Differences in Facial Skin Blood Flow Responses to Thermal Stimulation. *Eur. J. Appl. Physiol.* 5.1195-1201. <https://link.springer.com/article/10.1007/s00421-019-04109-6>.
- [85] Ahmed Cherif Megri, Issam El Naqa, Prediction of the thermal comfort indices using improved support vector machine classifiers and nonlinear kernel functions, *Indoor Built Environ.* 25 (1) (2016) 6–16. <https://journals.sagepub.com/doi/abs/10.1177/1420326X14539693>.
- [86] Giovanni Tardioli, Ricardo Filho, Pierre Bernaud, Dimitrios Ntimos, An innovative modelling approach based on building physics and machine learning for the prediction of indoor thermal comfort in an office building, *Buildings* 12 (4) (2022), <https://doi.org/10.3390/environsciproc2021011025>.
- [87] J. van Hoof, L.M. Jan, Mazej M. Fau - Hensen, J.L. Hensen, Thermal comfort: research and practice, 2768-6698. (Electronic), *Front. Biosci.* 15 (2) (2010), <https://doi.org/10.2741/3645>, 765–88.
- [88] Muhammad Fayyaz, Asma Ahmad Farhan, Abdul Rehman Javed, Thermal comfort model for hvac buildings using machine learning, *Arabian J. Sci. Eng.* 47 (2) (2022) 2045–2060, <https://doi.org/10.1007/s13369-021-06156-8>.
- [89] T. Liapikos, C. Zisi, D. Kodra, K. Kademoglou, D. Diamantidou, O. Begou, A. Pappa-Louisi, G. Theodoridis, Quantitative structure retention relationship (qsrr) modelling for analytes' retention prediction in Lc-Hrms by applying different machine learning algorithms and evaluating their performance, *J. Chromatogr. B* 1191 (2022) 123132. <https://www.sciencedirect.com/science/article/pii/S1570023222000368>.
- [90] Chan Jireh Yi-Le, Steven Mun Hong Leow, Khean Thye Bea, Wai-Khuen Cheng, Seul Wai Phoong, Zeng-Wei Hong, Yen-Lin Chen, Mitigating the multicollinearity problem and its machine learning approach: a review, *Mathematics* 10 (8) (2022) 1283. <https://www.mdpi.com/2227-7390/10/8/1283>.
- [91] Francesco Salamone, Alice Bellazzi, Lorenzo Belussi, Gianfranco Damato, Ludovico Danza, Federico Dell'Aquila, Matteo Ghellere, Valentino Megale, Italo Meroni, Vitaletti Walter, Evaluation of the visual stimuli on personal thermal comfort perception in real and virtual environments using machine learning approaches, *Sensors* 20 (6) (2020) 1627, <https://doi.org/10.3390/s20061627>.
- [92] Eddie Y.K. Ng, G.J.L. Kawb, W.M. Chang, Analysis of Ir thermal imager for mass blind fever screening, *Microvasc. Res.* 68 (2) (2004) 104–109. <https://www.sciencedirect.com/science/article/pii/S0026286204000548>.
- [93] Zi Wang, Hang Yu, Maohui Luo, Zhe Wang, Hui Zhang, Jiao Yu, Predicting older people's thermal sensation in building environment through a machine learning approach: modelling, interpretation, and application, *Build. Environ.* 161 (2019) 106231. <https://www.sciencedirect.com/science/article/pii/S036013231930441X>.
- [94] Sally Shahzad, John Brennan, Dimitris Theodossopoulos, John K. Calautit, Ben R. Hughes, Does a neutral thermal sensation determine thermal comfort? *Build. Serv. Eng.* 39 (2) (2018) 143–152, <https://doi.org/10.1177/0143624418754498>.